Three-Dimensional Structure of Tetrahydrodipicolinate *N*-Succinyltransferase[†,‡]

Todd W. Beaman, David A. Binder, John S. Blanchard, and Steven L. Roderick*

Department of Biochemistry, Albert Einstein College of Medicine, 1300 Morris Park Avenue, Bronx, New York 10461

Received October 8, 1996; Revised Manuscript Received November 18, 1996[⊗]

ABSTRACT: The conversion of tetrahydrodipicolinate and succinyl-CoA to *N*-succinyltetrahydrodipicolinate and CoA is catalyzed by tetrahydrodipicolinate *N*-succinyltransferase and is the committed step in the succinylase pathway by which bacteria synthesize L-lysine and *meso*-diaminopimelate, a component of peptidoglycan. The X-ray crystal structure of THDP succinyltransferase has been determined to 2.2 Å resolution and has been refined to a crystallographic *R*-factor of 17.0%. The enzyme is trimeric and displays the left-handed parallel β-helix (LβH) structural motif encoded by the "hexapeptide repeat" amino acid sequence motif [Raetz, C. R. H., & Roderick, S. L. (1995) *Science 270*, 997−1000]. The approximate location of the active site of THDP succinyltransferase is suggested by the proximity of binding sites for two inhibitors; *p*-(chloromercuri)benzenesulfonic acid and cobalt ion, both of which bind to the LβH domain.

The biosynthesis of L-lysine from L-aspartic acid in bacteria occurs via the DAP[1]/lysine pathway (Gilvarg & Weinberger, 1970). Gram-negative bacteria, gram-positive cocci, blue-green algae, and higher plants utilize tetrahydrodipicolinate *N*-succinyltransferase (THDP succinyltransferase) to form *N*-succinyl-THDP and CoA from succinyl-CoA and THDP in the central portion of this pathway (Scheme 1). The importance of L-lysine and the intermediate *meso*-DAP, a component of peptidoglycan, has drawn attention to this pathway and the THDP succinyltransferase in particular as potential targets for inhibitors directed against organisms utilizing this pathway. Studies of *Escherichia coli* THDP succinyltransferase have suggested a model for the reaction involving hydration of the imine group of THDP followed by succinylation and ring opening to yield the acyclic product *N*-succinyl-THDP (Berges et al., 1986) which may then be transaminated in the next step of the pathway. Inhibitors of this enzyme include the phenylmercurial PCMPS and various metal compounds, including $CoCl_2$ (Simms et al., 1984).

The gene encoding THDP succinyltransferase has been cloned from a plasmid library of *Mycobacterium bovis* BCG, overexpressed in *E. coli*, and sequenced (Binder et al., 1996). The inability of the cloned gene to hybridize to *M. bovis* genomic DNA suggested that the gene may have been amplified from contaminating DNA from a high G+C organism, perhaps another mycobacterial species. The inferred amino acid sequence of 274 residues is 94% identical to the *E. coli* enzyme (Richaud et al., 1984) and displays the imperfect tandem-repeated hexapeptide sequence of the "hexapeptide repeat" group of enzymes (Vuorio et al., 1991, 1994; Dicker & Seetharam, 1992). Most, though not all, enzymes of this group are acyltransferases and utilize a phosphopantothenyl-based substrate donor, either as acyl-CoA or the acyl-acyl carrier protein, whose prosthetic group closely resembles CoA. Enzymes of this group share amino acid sequence similarity as an imperfect tandem-repeated hexapeptide sequence, characterized as [LIV]-[GAED]-X_2-[STAV]-X in the hexapeptide repeat PROSITE database (Bairoch, 1993). This sequence has been shown to encode a left-handed parallel β helix in the three-dimensional structure of *E. coli* UDP-*N*-acetylglucosamine acyltransferase (LpxA) (Raetz & Roderick, 1995) and a carbonic anhydrase from the thermophilic archaeon *Methanosarcina thermophila* (Cam) (Kisker et al., 1996).

We recently reported the preparation of good quality single crystals of THDP succinyltransferase (Binder et al., 1996) and describe here the three-dimensional crystal structure of this enzyme refined to 2.2 Å resolution. In addition, the approximate location of the active site of this enzyme is suggested by the binding site locations of two inhibitors: PCMPS and cobalt ion.

EXPERIMENTAL PROCEDURES

Purification and Crystallization. THDP succinyltransferase was purified as previously described and crystallized from solutions of 16% (w/v) poly(ethylene glycol) 4000, 200 mM ammonium sulfate, 100 mM HEPES, pH 7.5, and 10% (v/v) 2-propanol (Binder et al., 1996). These crystals belong to space group $P2_1$ with unit cell parameters $a = 60.6$ Å, $b = 107.9$ Å, $c = 70.7$ Å, and $\beta = 113.0°$. The largest crystals usually appear as overlaid plates with approximate dimensions of $0.3 \times 0.6 \times 0.1$ mm and yield X-ray reflections to 2.2 Å resolution. Consideration of typical packing densities in protein crystals (Matthews, 1974) suggested the presence of one trimeric molecule (89 660 Da) in the asymmetric unit and a unit cell composed of approximately 48% solvent.

Data Measurement and MIR Phasing. Primary phases were determined by the method of isomorphous replacement using three heavy atom derivatives. X-ray diffraction data from three separate native crystals and one crystal for each

[†] This work was supported by Grants AI33696 (to J.S.B.) and AI38328 (to S.L.R.) and by the Mathers Foundation.

[‡] The coordinates of THDP succinyltransferase have been deposited in the Brookhaven Protein Data Bank (filename 1TDT).

* To whom correspondence should be addressed.

[⊗] Abstract published in *Advance ACS Abstracts,* January 1, 1997.

[1] Abbreviations: THDP, tetrahydrodipicolinate; DAP, diaminopimelate; CoA, coenzyme A; MIR, multiple isomorphous replacement; PCMPS, *p*-(chloromercuri)benzenesulfonic acid; RMS, root mean square; LβH, left-handed parallel β-helix; LpxA, *Escherichia coli* UDP-*N*-acetylglucosamine acyltransferase; Cam, *Methanosarcina thermophila* carbonic anhydrase.

S0006-2960(96)02522-6 CCC: $14.00

Scheme 1

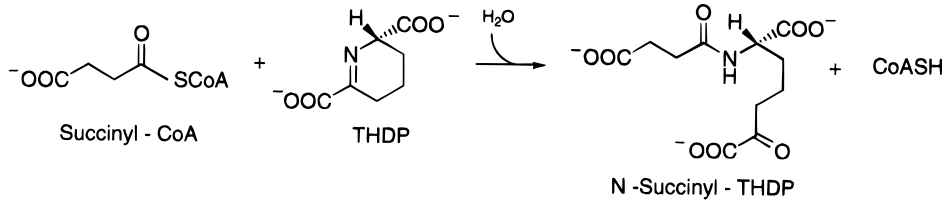

Table 1: Data Measurement Statistics[a]

data	observed	unique	completeness	R_{merge}	R_{iso}
native	137 056	38 447	0.90	0.067	
cis-$Pt(NH_3)_2Cl_2$ (I)	58 584	25 481	0.88	0.076	0.183
cis-$Pt(NH_3)_2Cl_2$ (II)	132 328	28 045	0.97	0.053	0.076
PCMPS	96 712	27 438	0.95	0.074	0.207
$CoCl_2$	75 931	19 498	0.94	0.071	0.108

[a] Data measurement statistics for THDP succinyltransferase employing native and three heavy atom derivatives and a crystal soaked in the inhibitor $CoCl_2$: *cis*-$Pt(NH_3)Cl_2$ (I) (2 mM; 1 day soak; freshly prepared solution), *cis*-$Pt(NH_3)Cl_2$ (II) (2 mM; 1 day soak; 1 week old solution), PCMPS [1 mM *p*-(chloromercuri)benzenesulfonic acid; 100 min soak], and $CoCl_2$ (1 mM; 4 h). The total number of observed reflections, the number of unique reflections, and the completeness of the data are given for the native data set (2.2 Å resolution measured from three crystals), the three derivative data sets (2.5 Å resolution; one crystal per data sets) and the $CoCl_2$ data (2.8 Å resolution; one crystal). The completeness of the native data set in the 2.3−2.2 Å shell was 0.73. $R_{merge} = \sum|I_i - \langle I\rangle|/\sum|I_i|$ within one data set, and $R_{iso} = \sum|F_{Nat} - F_{Der}|/\sum|F_{Nat}|$ between native and derivative data sets.

of three heavy metal derivatives were measured with a Siemens X1000 area detector mounted on a Rigaku RU200 rotating anode generator operating with fine focus at 50 kV and 80 mA. The data were reduced with the XDS program package (Kabsch, 1988) (Table 1). Analysis of difference Patterson functions with the program VERIFY (S. L. Roderick, unpublished program) and inspection of cross-phased difference Fourier maps revealed the presence of seven platinum sites in a crystal soaked in a freshly prepared solution of *cis*-$Pt(NH_3)_2Cl_2$. A second crystal that had been soaked in the same solution the following week for a similar time bound platinum at just three sites. A PCMPS derivative crystal yielded three distinct mercury binding sites. The PHASES program package (Furey & Swaminathan, 1995) was used to conduct heavy atom parameter refinement, MIR phase calculation, and solvent flattening procedures, all with 2.5 Å resolution data (Table 2). Maps calculated with and without each *cis*-$Pt(NH_3)_2Cl_2$ derivative data set were inspected, and the map calculated with both platinum data sets was preferred and used for further work. The mean figure of merit of the phase calculation to 2.5 Å resolution was 0.61.

A self-rotation function calculated with the program GLRF (Tong & Rossmann, 1990) suggested the presence of a 3-fold axis of rotation within the asymmetric unit of these crystals (data not shown), and it indeed proved possible to relate the three mercury binding sites and two triplets of platinum sites by this 3-fold rotation axis (Table 2). The angular orientation and translation of this axis were then refined against the electron density of a 2.8 Å MIR map within the PHASES program suite (program LSQROT). This yielded a correlation coefficient of electron density values between different subunits of 0.66 and served to define the coordinate transformations that were then used to average a solvent-flattened 2.5 Å electron density map for use in model building.

Model Building and Atomic Parameter Refinement. The high quality of the final solvent-flattened and 3-fold averaged 2.5 Å resolution electron density map supported an immediate polypeptide chain trace using the graphics program O (Jones et al., 1991). This trace included 255 of 274 residues within a single averaged subunit of electron density. Electron density corresponding to the N-terminal two residues and the C-terminal 17 residues was of lower quality or absent, and so these residues were initially omitted from the model. The coordinate transformations that were used to average the electron density map were then used to rotate the coordinates of the single-subunit atomic model into the remaining two subunit locations of the trimer. From this point forward, no use was made of the 3-fold noncrystallographic symmetry except for the occasional calculation and inspection of averaged $2F_o - F_c$ and $F_o - F_c$ maps in an effort to interpret ambiguous density.

Approximately 5% of the diffraction data were assigned to a test set and omitted from the initial refinement procedures in order to calculate the ordinary working set residual R_{work} and the cross-validation statistic R_{free} (Brunger, 1992; Kleywegt & Brunger, 1996). In later stages, R_{free} was calculated *a posteriori* using simulated annealing refinements starting at 4000 K to uncouple the working and free *R* values (Kleywegt & Brunger, 1996). R_{work} for the prerefined model of the trimeric enzyme (5583 atoms) was 32.7% for all unique data in the 6.0−3.5 Å resolution range of the working set (R_{free} 35.9%). Refinement of this model as 12 rigid body fragments was carried out using the X-PLOR program package (Brunger et al., 1990) with all unique 6.0−3.5 Å data of the work set (R_{work} 32.0%, R_{free} 35.5%) and followed by a simulated annealing refinement of atomic positional parameters using all unique data in the 6.0−2.5 Å resolution range of the work set (R_{work} 24.1%, R_{free} 34.1%). This model was rebuilt by inspection of $2F_o - F_c$ and $F_o - F_c$ maps and in the process 75 well-defined water molecules were added. The conjugate direction procedures encoded in the TNT suite of computer programs (Tronrud et al., 1987) were then used to refine individual positional and thermal parameters for protein and solvent atoms as well as a solvent continuum model using all unique data to 2.3 Å (*R*-factor 18.0%, *a posteriori* R_{free} 24.3%). Further model building and refinement cycles using all unique data to 2.2 Å resolution (0.90 complete, 0.73 complete in the 2.3−2.2 Å shell) resulted in an *a posteriori* R_{free} of 23.2% and a final crystallographic *R*-factor of 17.0%.

Location of Inhibitors. The heavy metal compound PCMPS was used both to calculate MIR phase angles and to locate the active site, since it also is an inhibitor of the THDP succinyltransferase from *E. coli* (Simms et al., 1984). To examine the binding of cobalt ion, also an inhibitor, a crystal was soaked in 16% (w/v) poly(ethylene glycol) 4000, 200 mM ammonium sulfate, 100 mM HEPES, pH 7.5, and 10% (v/v) 2-propanol containing 1 mM $CoCl_2$ for 4 h, and

Table 2: Heavy Atom Parameter Refinement and Phase Calculation Statistics[a]

derivative	site	occ	*X*	*Y*	*Z*	*B*	f_c/LOC	R_c
cis-$Pt(NH_3)_2Cl_2$ (I)	A1	1.00	−0.0665	0.0025	−0.0126	21.1	2.14	0.54
	A2	0.98	0.1608	−0.1093	−0.1949	22.4		
	A3	0.93	−0.2258	−0.0283	−0.3964	23.2		
	B1	0.83	0.2097	−0.0830	−0.2788	24.7		
	B2	0.85	0.0617	0.0414	0.0613	20.2		
	B3	0.96	−0.3102	0.0463	−0.4129	19.1		
	C	0.87	−0.5093	−0.3568	−0.0216	22.9		
cis-$Pt(NH_3)_2Cl_2$ (II)	B1	0.82	0.2040	−0.0830	−0.2959	22.6	1.62	0.62
	B2	0.93	0.0688	0.0370	0.0651	16.1		
	B3	0.97	−0.3139	0.0461	−0.4086	15.1		
PCMPS	D1	0.93	−0.2007	0.0577	−0.0238	18.0	1.63	0.60
	D2	0.70	0.3153	−0.1060	−0.0610	18.6		
	D3	0.58	−0.2280	−0.0472	−0.5264	18.5		
overall figure of merit for 26 345 reflections (0.91 complete) to 2.5 Å = 0.61								

[a] The refined relative occupancies, fractional coordinates, and thermal factors (Å^2) resulting from the 2.5 Å heavy atom parameter refinement and isomorphous replacement phase calculation. f_c/LOC = RMS heavy atom structure factor amplitude/RMS lack of closure. $R_c = \sum||f_{H,obs}| - |f_{H,calc}||/\sum||f_{H,obs}||$ for the 567, 637, and 453 centric reflections measured from the three heavy atom derivative crystals. Heavy atom site names beginning with the same letter occupy chemically equivalent positions in the three subunits of the trimeric enzyme.

X-ray data were then measured to 2.8 Å resolution (Table 1). Difference Fourier coefficients constructed using phases of the refined model were transformed, and the resulting map was inspected using molecular graphics.

RESULTS AND DISCUSSION

Atomic Model of THDP Succinyltransferase. The model of THDP succinyltransferase consists of atoms corresponding to residues 1−256, 2−256, and 4−256 of the three subunits of the trimeric enzyme (5780 atoms) and additionally contains 215 solvent molecules, all modeled as water. The C-terminal 18 residues were not well-defined in any subunit and could not be modeled adequately. The side chains of an additional 17 residues were truncated to alanine due to weak electron density.

The stereochemical quality of the model is very good, with RMS deviations of bond lengths and bond angles from ideality of 0.009 Å and 1.97°. The program PROCHECK (Laskowski et al., 1993) was used to monitor the quality of the model, which was found to be within ordinary bounds or better in all geometric categories as compared to other structures refined at similar resolution. A Ramachandran plot of main-chain torsion angle pairs ϕ and ψ for all residues shows that 90% are placed in the energetically most favored region of the plot with no non-glycine residues in the generously allowed or disallowed regions (Figure 1). The final refined model is also sterically and chemically consistent with the location of the heavy metal binding sites used in MIR phasing. The three PCMPS sites bind to Cys 149 in each subunit of the trimer, and the two triplets of platinum sites in the first *cis*-$Pt(NH_3)_2Cl_2$ derivative bind near Met 124 and His 157. The seventh platinum site of this derivative binds in a unique location between two trimers. The second *cis*-$Pt(NH_3)_2Cl_2$ derivative crystal, which had been soaked in an aged heavy atom solution, binds platinum only to His 157 in each of three subunits, perhaps due to a time-dependent oxidation or ligand exchange reaction that altered the reactivity of this heavy metal compound.

Polypeptide Chain Fold. An α-carbon backbone diagram of THDP succinyltransferase is shown in Figure 2. The asymmetric unit of the monoclinic crystals contains one trimeric molecule, which is composed of three chemically identical subunits related by a 3-fold rotation axis. This is in contrast to a prediction that this enzyme is dimeric, as

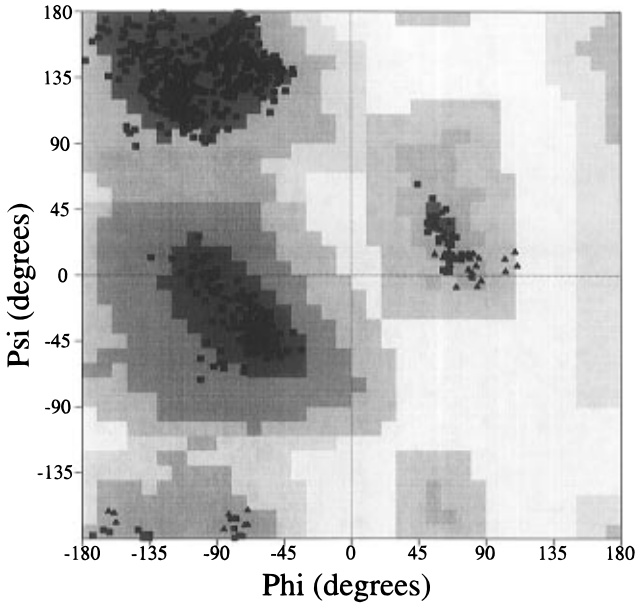

FIGURE 1: Ramachandran diagram (Ramachandran et al., 1963) of the main-chain torsion angles ϕ and ψ for the refined model of THDP succinyltransferase. The shading indicates levels of conformational energy for non-glycine residues with white signifying energetically forbidden regions. Glycine residues are depicted as filled triangles (▲). Figure based on output from PROCHECK (Laskowski et al., 1993).

judged by gel filtration and sucrose density gradient centrifugation data (Simms et al., 1984). The overall dimensions of the trimer present in these crystals are approximately 60 × 60 × 56 Å. The structure of a single subunit of the enzyme is formed by three domains (Figure 3). An N-terminal domain corresponding to residues 1−101 contains four α-helices in the ranges of 2−13, 24−40, 57−70, and 94−101 and two twisted hairpin loops (residues 45−56 and 73−84). The second domain (residues 102−233) is predominantly composed of a coiled parallel β-sheet and contains *cis*-peptide bonds preceding Pro 108 and Pro 170. This β-structure is interrupted at two locations by external loops corresponding to residues 166−175 and 210−224. The portion of the C-terminal domain that is included in the current refined model (residues 234−256) is of mostly β-structure and caps the C-terminal end of the coiled parallel β-domain. Intermolecular contacts that produce the monoclinic crystal form studied here are formed predominantly

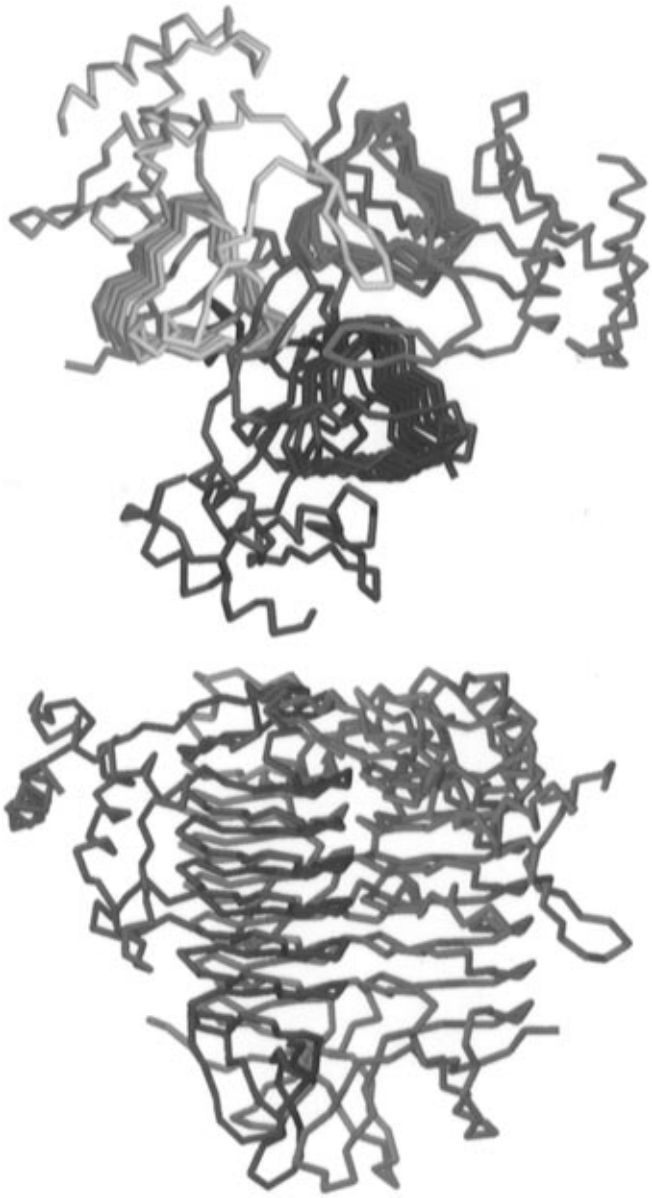

FIGURE 2: α-Carbon diagrams of the trimeric enzyme. (A, top) View nearly parallel to the molecular 3-fold axis that relates the three subunits. (B, bottom) View nearly perpendicular to the 3-fold axis. This figure and Figures 4 and 6 produced by SETOR (Evans, 1993).

by interactions between the N-terminal domains of separate trimers.

The three-dimensional structure of THDP succinyltransferase is dissimilar to other proteins in a structural database according to comparison routines encoded in the DALI protein structure similarity server (Holm & Sander, 1993) except in the parallel β-domain (see below).

Structure of the Left-Handed Parallel β-Helix (LβH). Perhaps the most striking feature of the three-dimensional structure of the enzyme is the appearance of the left-handed parallel β-helix (LβH) structural motif of residues 102−233 in each subunit (Raetz & Roderick, 1995) (Figures 2 and 3). This structural domain corresponds to the imperfect tandem-repeated hexapeptide sequence and folds as a large coiled prism as if wound in a left-handed spiral around the surface of an equilateral prism. The axis of each LβH is nearly parallel to the 3-fold axis that relates subunits of the trimer (Figure 2).

The helical nature of this domain places successive triangular coils, each composed of three hexapeptide units, on top of one another in nearly identical orientations that promote several different types of repetitive interactions between structurally equivalent residues of adjacent coils (Figure 4). The flat faces of the LβH are parallel β-sheets formed by short β-strands. Typically, two residues per strand adopt main-chain ϕ and ψ angles characteristic of β-structure and fully participate in the interstrand main-chain hydrogen bonding of backbone amide and carbonyl groups. These hydrogen bonds are confined to the flat faces of the LβH. The β-strands, termed PB1, PB2, and PB3, are separated by either tight turns (T1, T2, T3) or external loops that project outward from the LβH. The tight turns are flat and orient the central peptide plane perpendicular to the plane of the turn. The main-chain torsion angles of residues flanking the central peptide unit are similar to those of classical type II turns (Richardson, 1981) with the main-chain amide and carbonyl groups of the central peptide unit frequently hydrogen bonded to similar groups in the turns of adjacent coils. The narrow central channel that runs collinear with the axis of the prismatic LβH domain is too narrow to accommodate solvent.

The alignment of structurally equivalent residues in adjacent coils is demonstrated in the structure-based amino acid sequence alignment (Figure 5). The conserved aliphatic residue at position *i* (Leu, Ile, Val) of the hexapeptide repeat sequence motif ([LIV]-[GAED]-X_2-[STAV]-X) projects into the interior of the LβH (Figure 4). Val and Ile residues at this position adopt a staggered side-chain conformation with respect to the main chain and exhibit cupped stacking in columns with the structurally equivalent residues of adjacent coils. Residues at position $i + 4$ include Ser, Thr, Ala, and Val of the hexapeptide repeat sequence motif but also Cys (in LpxA, Cam, and THDP succinyltransferase) and Asn (LpxA). The side chains of these small residues project into the interior of the LβH at the triangular corners of each coil and are subject to steric constraints. Both polar and nonpolar residues can be accommodated at this position since polar residues (Ser, Cys, Thr) form hydrogen bonds to main-chain peptide groups of the tight turn in the succeeding coil while nonpolar residues (Ala, Val) do not disrupt hydrogen bond formation between these peptide groups across the tight turns of these coils. In addition to these sequence determinants, a significant structural characteristic of the LβH domain is the presence of a residue at position $i + 3$ that projects outward from the LβH. This residue frequently adopts a left-handed conformation (main-chain torsion angle $\varphi > 0°$ in 14 of 15 positions).

Subunit−Subunit Interactions. The overall conformations of each subunit are very nearly identical. The RMS deviation of equivalent C_α atoms after least squares superposition is 0.27, 0.32, and 0.25 Å for the three subunit pairs of the trimer. The association between subunits is very intimate and buries approximately 3260 Å^2 (27%) of the contact area of each subunit in the trimeric enzyme. The interactions between subunits involve residues from each of the three domains, most often at or close to the 3-fold rotation axis. Intersubunit interactions from the N-terminal domain primarily involve residues in a hairpin loop (residues 73−84) that covers the first T2 turn of an adjacent subunit. The LβH contributes subunit−subunit interactions with side chains from its column of T2 turns and those of the flat PB3 face of an adjacent subunit as well as hydrophobic and hydrophilic residues surrounding the 3-fold rotation axis. The C-terminal domain participates in intersubunit interactions

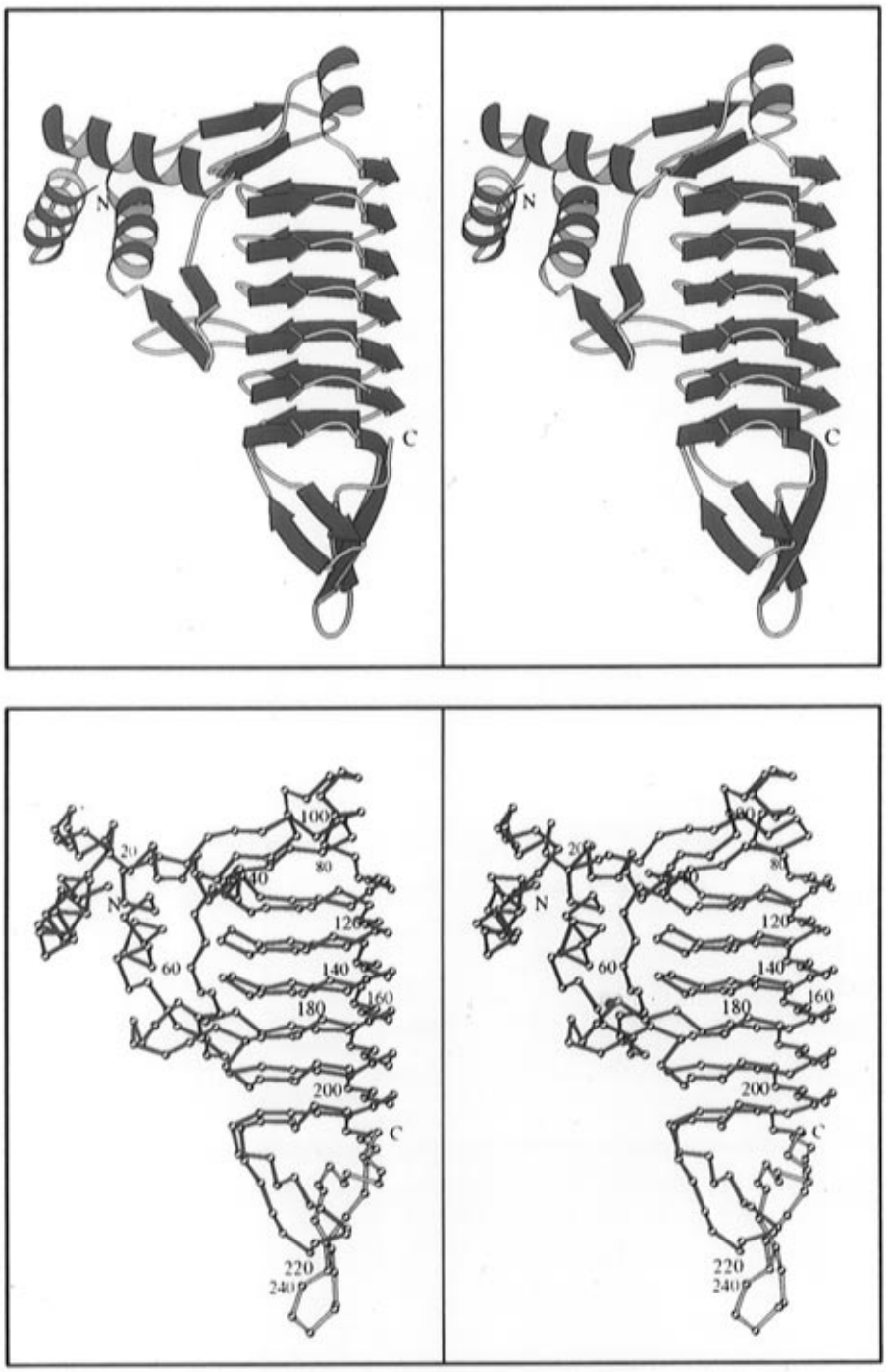

FIGURE 3: Stereoviews of a single subunit of THDP succinyltransferase. (Top panel) Ribbon diagram depicting the α-helical (red) and β-strand (blue) secondary structure. (Bottom panel) α-Carbon diagram depicting the domain structure. The domains are N-terminal (red), left-handed β-helix (blue), and C-terminal (yellow). External loops projecting from the β-helix are shown in green. Figure produced by MOLSCRIPT (Kraulis, 1991).

with residues 236−248 which form a hairpin loop that runs nearly parallel and very close to the 3-fold rotation axis, resulting in a small six-stranded β-type antiparallel structure involving strands from all three subunits.

Location of Inhibitor Binding Sites. The precise location of the active site of THDP succinyltransferase is not known nor have catalytically important residues been defined. However, studies with the enzyme from *E. coli* indicate that the phenylmercurial compound PCMPS completely inhibits the enzyme and that 1 mM $CoCl_2$ inhibits enzyme activity by ~95% (Simms et al., 1984). The three PCMPS sites were located in the course of MIR phasing procedures and were found to bind Cys 149 in each of the three subunits. This residue is contained in the T3 turn of the third coil and is located directly over the first external loop that projects outward from the LβH (residues 166−175). In order to locate potential cobalt ion binding sites, a crystal was soaked in a solution containing 1 mM $CoCl_2$ for 4 h and X-ray diffraction data were measured (Table 1). Difference Fouriers indicate that four Co^{2+} ions are bound. Three of these sites are present in chemically equivalent positions of the trimer and are bound by the side-chain carboxylate of Asp 141 (OD2−Co^{2+}; 2.4 Å) and the imidazole ring of His 157 (NE2−Co^{2+}; 2.3 Å) from residues that belong to the LβH of the same subunit. The fourth cobalt binding site is located directly on the molecular 3-fold rotation axis and interacts via water molecules with the side-chain carboxylate of Glu 79 of each subunit from the N-terminal domain. All of the

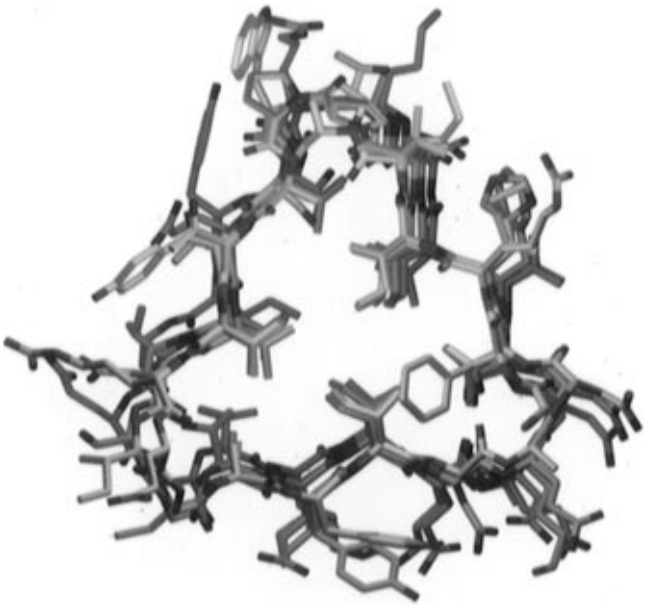

FIGURE 4: Left-handed parallel β-helix (LβH) domain. Residues 102−165, 176−209, and 225−233 are shown. The conserved aliphatic residues (Leu, Ile, Val) at position *i* and the conserved small residues at position $i + 4$ (Ala, Ser, Cys, Val, Thr) that point toward the interior of the LβH are visible.

		PB1				T1		PB2			T2		PB3			T3		
C1	102						**G**	F	R	V	V	P	P	A	T	V	R	Q **G**	114
C2	115	A	F	I	A	R	**N**	T	V	L	M	P	-	S	Y	V	N	I **G**	131
C3	132	A	Y	V	D	E	**G**	T	M	V	D	T	**W**	A	T	V	G	S **C**	149
C4	150	A	Q	I	G	K	**N**	V	H	L	S	G	**G**	V	G	I	G	Loop 1	165
C5	176	T	I	I	E	D	**N**	C	F	I	G	A	**R**	S	E	V	V	E **G**	193
C6	194	V	I	V	E	E	**G**	S	V	I	S	M	**G**	V	Y	L	G	Loop 2	209
C7	225	G	R	V	P	A	**G**	S	V	V									233

FIGURE 5: Structure-based amino acid sequence alignment of the LβH domain of THDP succinyltransferase (residues 102−233) identifying structurally equivalent residues in each of the seven coils. The three-dimensional structure of this region is shown in Figure 4. Each horizontal line represents one complete or partial coil. The parallel β-strands that form the planar faces of the LβH are denoted PB1, PB2, and PB3 and the turns separating these strands T1, T2, and T3. The conserved aliphatic residues at position *i* are boxed. Residues in left-handed conformation (main-chain torsion angle $\varphi > 0$) at position $i + 3$ are depicted in bold type. The small residues at the corners of each coil at position $i + 4$ are reverse shaded. The location of the two external loops (166−175 and 210-224) that project from the LβH is also indicated.

residues that interact with the PCMPS and Co^{2+} inhibitors are conserved in the sequence of the *E. coli* THDP succinyltransferase (Richaud et al., 1984). The PCMPS and cobalt binding sites that are in closest proximity to one another (interatomic distance 11.9 Å) are bound by side chains from the PB2 face of one subunit (Asp 141 and His 157) and the T3 turn of an adjacent subunit (Cys 149). The pairwise proximity of six of the seven inhibitor binding sites (three PCMPS, three Co^{2+}) related in this way suggests that the active sites of THDP succinyltransferase could be located at the junction between subunits of the trimer in an open cleft that is large enough to accommodate substrates and is bounded by the planar faces of the LβH domains of two separate subunits.

ACKNOWLEDGMENT

The authors gratefully acknowledge Drs. Massimo Degano and Giovanna Scapin for helpful discussions. The *E. coli* strain expressing the THDP succinyltransferase was constructed by Renjian Zheng in the Department of Biochemistry of the Albert Einstein College of Medicine.

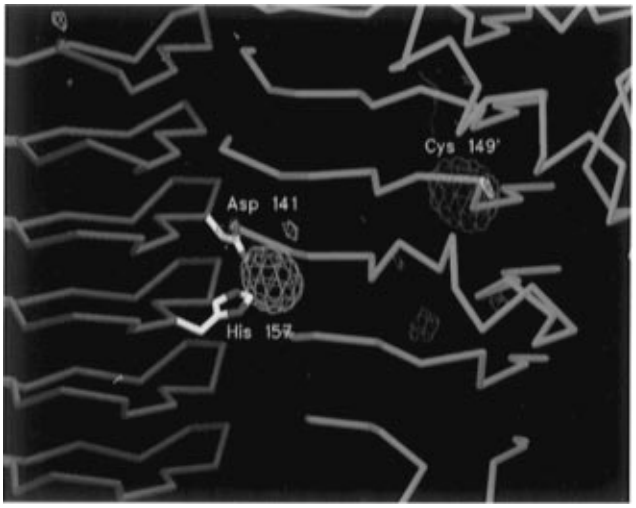

FIGURE 6: Diagram indicating the location of a single pair of bound PCMPS and cobalt ion inhibitors of THDP succinyltransferase. The difference Fourier electron density corresponding to the PCMPS (red) and $CoCl_2$ (blue) inhibitors is shown. The direction of view is similar to that of Figure 2B and depicts portions of two different subunits.

REFERENCES

Bairoch, A. (1993) *Nucleic Acids Res. 21*, 3097−3103.
Berges, D. A., DeWolf, Jr., Dunn, G. L., Newman, D. J., Schmidt, S. J., Taggart, J. J., & Gilvarg, C. (1986) *J. Biol. Chem. 261*, 6160−6167.
Binder, D. A., Blanchard, J. S., & Roderick, S. L. (1996) *Proteins 26*, 115−117.
Brunger, A. T. (1992) *Nature 355*, 472−475.
Brunger, A. T., Krukowski, A., & Erickson, J. W. (1990) *Acta Crystallogr. A46*, 585−593.
Dicker, I. B., & Seetharam, S. (1992) *Mol. Microbiol. 6*, 817−823.
Evans, S. V. (1993) *J. Mol. Graphics 11*, 134−138.
Furey, W., & Swaminathan, S. (1995) American Crystallographic Association Meeting Program Abstract, 18, 73.
Gilvarg, C., & Weinberger, S. (1970) *J. Bacteriol. 101*, 323−324.
Holm, L., & Sander, C. (1993) *J. Mol. Biol. 233*, 123−138.
Jones, T. A., Zou, J.-Y., Cowan, S. W., & Kjeldgaard, M. (1991) *Acta Crystallogr. A47*, 110−119.
Kabsch, W. (1988) *J. Appl. Crystallogr. 21*, 916−924.
Kisker, C., Schindelin, H., Alber, B. E., Ferry, J. G., & Rees, D. C. (1996) *EMBO J. 15*, 2323−2330.
Kleywegt, G. J., & Brunger, A. T. (1996) *Structure 4*, 897−904.
Kraulis, P. J. (1991) *J. Appl. Crystallogr. 24*, 946−950.
Laskowski, R. A., MacArthur, M. W., Moss, S. D., & Thornton, J. M. (1993) *J. Appl. Crystallogr. 26*, 283−291.
Matthews, B. W. (1974) *J. Mol. Biol. 82*, 513−526.
Raetz, C. R. H., & Roderick, S. L. (1995) *Science 270*, 997−1000.
Ramachandran, G. N., Ramakrishnan, C., & Sasisekharan, V. (1963) *J. Mol. Biol. 7*, 95−99.
Richardson, J. S. (1981) *Adv. Protein Chem. 34*, 167−339.
Richaud, C., Richaud, F., Martin, C., Haziza, C., & Patte, J. C. (1984) *J. Biol. Chem. 259*, 14824−14828.
Simms, S. A., Voige, W. H., & Gilvarg, C. (1984) *J. Biol. Chem. 259*, 2734−2741.
Tong, L., & Rossmann, M. G. (1990) *Acta Crystallogr. A46*, 783−792.
Tronrud, D. E., Ten Eyck, L. F., & Matthews, B. W. (1987) *Acta Crystallogr. A43*, 489−501.
Vuorio, R., Hirvas, L., & Vaara, M. (1991) *FEBS Lett. 292*, 90−94.
Vuorio, R., Harkonen, T., Tolvanen, M., & Vaara, M. (1994) *FEBS Lett. 337*, 289−292.

BI962522Q